Supplemental Information

Multidimensional Profiling Platforms Reveal Metabolic Dysregulation caused by Organophosphorus Pesticides

Daniel Medina-Cleghorn[1], Ann Heslin[1], Patrick Morris[1], Melinda M. Mulvihill[1], and Daniel K. Nomura[1]*

[1] Department of Nutritional Sciences and Toxicology, University of California, Berkeley, 127 Morgan Hall, Berkeley, CA 94720

*correspondence to dnomura@berkeley.edu

Supplemental Methods

Chemicals. OP pesticides were purchased from Sigma, Santa Cruz Biotechnology, and ChemService. Synthetic substrates were purchased from Avanti Polar Lipids and Sigma. FP-rhodamine and FP-biotin were synthesized based on previously established procedures (*1*). Selective serine hydrolase inhibitors JZL184, JZL195, and PF3485 were purchased from Cayman Chemical or synthesized based on previously established procedures (*2, 3*). Phosphatase and phospholipase D inhibitors were purchased from Cell Signaling Technology (100x Phosphatase Inhibitor Cocktail 5870S) and Sigma (5-fluoro-2-indolyl des-chlorohalopermide).

Mice. C57BL/6 male mice (6 weeks old) were exposed by intraperitoneal injection with each pesticide in a vehicle of 18:1:1 saline/emulphor/ethanol (10μl/g mouse). The maximally tolerated dose for each pesticide was selected based on previously reported conditions and on conditions established in these experiments. Mice were treated with 10 mg/kg EPF, 30 mg/kg PBF, 50 mg/kg CPF, 100 mg/kg TBF or 100 mg/kg PB. After 4 h, mice were sacrificed by cervical dislocation and brains, livers, lungs, kidneys, and testes were removed and flash frozen in liquid nitrogen. $MGLL^{+/+}$ and $MGLL^{-/-}$ mice described previously (*4*), were on a mixed genetic background of C57BL/6 and 129Sv and were obtained from The Scripps Research Institute. Animal experiments were conducted in accordance with the guidelines of the Institutional Animal Care and Use Committee of the University of California, Berkeley.

Cell Culture and Recombinant Overexpression Conditions. HEK293T cells were cultured in DMEM media containing 10% FBS and maintained at 37^{o}C with 5% CO_2. Recombinant cDNA constructs containing enzymes of interest in the SPORT6 vector were purchased from Thermo Open Biosystems and transiently transfected into HEK293T cells using Fugene.

ABPP of Mouse Tissue Proteomes and Recombinantly Overexpressed Enzyme. Tissues were homogenized in phosphate-buffered saline (PBS), followed by a 1000 x *g* centrifugation of the homogenate. The resulting supernatant was collected and used for subsequent assays. For gel-based ABPP experiments in tissue, proteomes (50 μg) were incubated with FP-rhodamine (2 μM) for 30 min at room temperature in a 50 μL reaction volume. For gel-based ABPP experiments in overexpressed enzyme lysate, the following total protein amounts were selected based experimentally on achieving optimal resolution in gel: FAAH and MGLL, 5 μg; ABHD6, CES2C, ES1, and IAH1, 10 μg; AADAC, KIAA1363, and LIPE, 25 μg; ABHD3, ACHE, APEH, CES1G, and CES3B 50 μg. Inhibition of proteome or enzyme was achieved by pre-incubating the protein with inhibitor for 30 min at 37ºC, and then incubating with FP-rhodamine for 30 min at room temperature, except for overexpressed KIAA1363 which was pre-incubated with CPO for 5 min and labeled with FP-rhodamine for 15 min, due to our previous studies showing that KIAA1363 actively hydrolyzes CPO (*5*). The

reaction was quenched by the addition of 30 μL of 4 x SDS-PAGE loading buffer and heated at 90°C for 10 min. Samples were run on a 10% SDS-PAGE gel and scanned using a Typhoon flatbed fluorescence scanner (GE Healthcare). Activity of each enzyme was quantitated by measuring the density of the fluorescent gel band using Image J software.

ABPP-MudPIT analysis was performed using previously established procedures. Briefly, proteomes (1 mg tissue homogenate) were labeled with FP-biotin (5 μM) in 1ml PBS for 1 h at room temperature, solubilized in 1 % Triton X-100 for 1 h, denatured, and labeled enzymes were enriched using avidin beads, reduced and alkylated, and trypsinized. Tryptic peptides were analyzed on nanospray Thermo LTQ-XL MS/MS system in a data-dependent manner and MS2 files were analyzed subsequently by SEQUEST as previously described (*6*). We then filtered the subsequent list for serine hydrolases based on previous profiling of serine hydrolases with the FP-biotin probe in various tissues (*7*).

Metabolomic profiling. Nonpolar lipid metabolites were extracted in 3 ml of a 2:1 chloroform:methanol and 1 ml of PBS with inclusion of internal standards C12:0 dodecylglycerol (10 nmol) and pentadecanoic acid (10 nmol). Organic and aqueous layers were separated by centrifugation at 1000 x g for 5 min and the organic layer was collected, dried down under N_2 and dissolved in 120 μl chloroform. Metabolites were then chromatographically separated by liquid chromatography as previously described (*8*). MS analysis was performed with an electrospray ionization (ESI) source on an Agilent 6430 QQQ LC-MS/MS. The

capillary voltage was set to 3.0 kV, and the fragmentor voltage was set to 100 V. The drying gas temperature was 350^{o}C, the drying gas flow rate was 10 l/min, and the nebulizer pressure was 35 psi. Representative metabolites were quantified by SRM of the transition from precursor to product ions at associated optimized collision energies as previously described (*8*). Untargeted LC-MS was performed by scanning a mass range of m/z 50-1200 and data was exported as mzdata files and uploaded to XCMSOnline (xcmsserver.nutr.berkeley.edu) (*9*) to identify metabolites that were differentially changed. These metabolites from untargeted analysis were putatively identified through using the METLIN online database (*10*). Standards were purchased to confirm coelution and fragmentation of the standard with the metabolite of interest. These metabolites were then quantified by SRM analysis. Metabolites were quantified by integrating the area under the peak and were normalized to internal standard values and adjusted based on external standard curves, and then levels were expressed as relative levels compared to controls.

Hydrolytic Activity Assays

Activity assays were performed as previously described (*6*). Briefly, cell or tissue lysates (160 μg) in PBS were incubated with 10 or 100 μM lipids at 37ºC for 30 min in a volume of 400 μl before quenching with 1200 μl 2:1 chloroform:methanol and subsequent addition of 10 nmol of pentadecanoic acid or 10 nmol dodecylglycerol internal standards. Inhibitors (1 μM) were pre-incubated with proteomes for 30 minutes at 37ºC before addition of lipid substrate; phosphatase

inhibitors were incubated for 15 minutes at 37ºC prior to incubation with selective MGLL and/or FAAH inhibitors. The products were extracted into the organic layer, which was dried under nitrogen, dissolved in 120 µl chloroform, and directly injected into LC-MS/MS. Product levels were quantified by measuring the area under the peak and normalized in relation to internal standard levels.

Supplemental Table Legends

Table S1. ABPP-MudPIT data from pesticide-treated mice. Raw data from ABPP-MudPIT experiments. Individual replicates, averages, sems, and p-values are shown. Serine hydrolase activities are quantified by spectral counting. Each tab contains the serine hydrolase activities from vehicle- versus pesticide-treated mice in brain, liver, kidney, lung, and testes.

Table S2. Targeted metabolomic analysis of CPF-treated mice. Raw data from targeted metabolomic analysis. Data is shown as relative metabolite levels in relation to vehicle-treated controls. Each tab contains the metabolite levels for vehicle-treated brain and liver.

Supplemental Figures

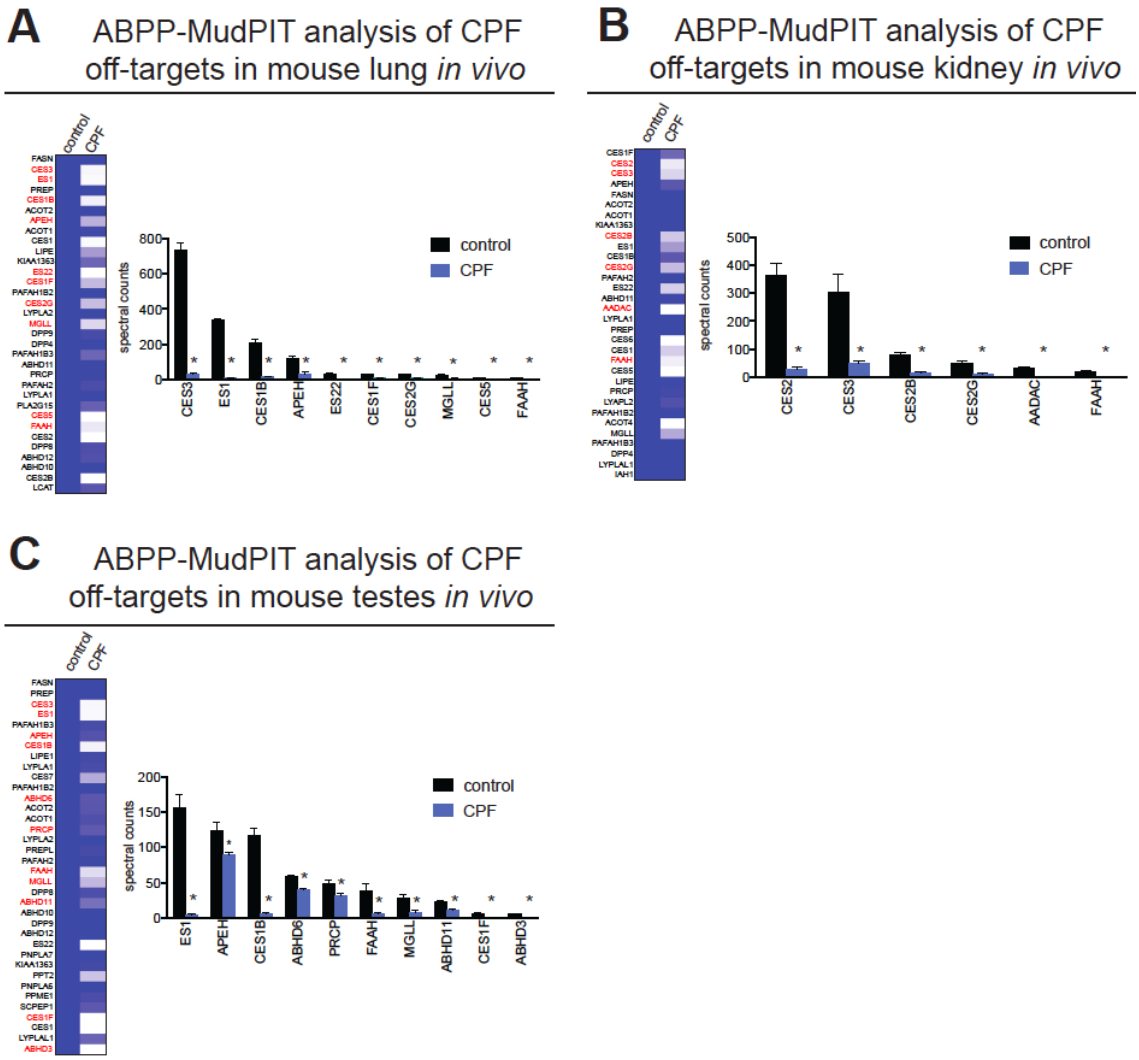

Figure S1. Functionally Inhibited Serine Hydrolase Off-Targets of CPF in Peripheral Tissues

(A) In mouse lung following *in vivo* exposure to CPF, 10 off-target serine hydrolases consisting primarily of CESs are functionally inhibited, (B) in mouse kidney, CPF exposure inhibits six, mostly CES off-targets, and (C) in mouse testes, 10 serine hydrolase off-targets are found to be inhibited by CPF *in vivo*,

though the majority of these off-targets in testes are poorly or incompletely characterized with respect to substrate and overall metabolic function. Darker blue shading on the heat map corresponds to relatively higher levels of activity, whereas lighter blue or white shading indicates lower activity. Data in A-C are presented as mean ± SEM; n= 3-4 per group. Significance is expressed in *A*-C as * $P < 0.05$ compared with vehicle-treated controls.

Supplemental References

1. Liu, Y., Patricelli, M. P., and Cravatt, B. F. (1999) Activity-based protein profiling: the serine hydrolases, *Proceedings of the National Academy of Sciences of the United States of America 96*, 14694-14699.
2. Long, J. Z., Nomura, D. K., Vann, R. E., Walentiny, D. M., Booker, L., Jin, X., Burston, J. J., Sim-Selley, L. J., Lichtman, A. H., Wiley, J. L., and Cravatt, B. F. (2009) Dual blockade of FAAH and MAGL identifies behavioral processes regulated by endocannabinoid crosstalk in vivo, *Proceedings of the National Academy of Sciences of the United States of America 106*, 20270-20275.
3. Long, J. Z., Nomura, D. K., and Cravatt, B. F. (2009) Characterization of monoacylglycerol lipase inhibition reveals differences in central and peripheral endocannabinoid metabolism, *Chemistry & biology 16*, 744-753.
4. Schlosburg, J. E., Blankman, J. L., Long, J. Z., Nomura, D. K., Pan, B., Kinsey, S. G., Nguyen, P. T., Ramesh, D., Booker, L., Burston, J. J., Thomas, E. A., Selley, D. E., Sim-Selley, L. J., Liu, Q. S., Lichtman, A. H., and Cravatt, B. F. (2010) Chronic monoacylglycerol lipase blockade causes functional antagonism of the endocannabinoid system, *Nature neuroscience 13*, 1113-1119.
5. Nomura, D. K., Leung, D., Chiang, K. P., Quistad, G. B., Cravatt, B. F., and Casida, J. E. (2005) A brain detoxifying enzyme for organophosphorus nerve poisons, *Proceedings of the National Academy of Sciences of the United States of America 102*, 6195-6200.
6. Nomura, D. K., Long, J. Z., Niessen, S., Hoover, H. S., Ng, S. W., and Cravatt, B. F. (2010) Monoacylglycerol lipase regulates a fatty acid network that promotes cancer pathogenesis, *Cell 140*, 49-61.
7. Bachovchin, D. A., Ji, T., Li, W., Simon, G. M., Blankman, J. L., Adibekian, A., Hoover, H., Niessen, S., and Cravatt, B. F. (2010) Superfamily-wide portrait of serine hydrolase inhibition achieved by library-versus-library screening, *Proceedings of the National Academy of Sciences of the United States of America 107*, 20941-20946.
8. Benjamin, D. I., Cozzo, A., Ji, X., Roberts, L. S., Louie, S. M., Mulvihill, M. M., Luo, K., and Nomura, D. K. (2013) Ether lipid generating enzyme AGPS alters the balance of structural and signaling lipids to fuel cancer pathogenicity, *Proceedings of the National Academy of Sciences of the United States of America 110*, 14912-14917.
9. Tautenhahn, R., Patti, G. J., Rinehart, D., and Siuzdak, G. (2012) XCMS Online: a web-based platform to process untargeted metabolomic data, *Analytical chemistry 84*, 5035-5039.
10. Tautenhahn, R., Cho, K., Uritboonthai, W., Zhu, Z., Patti, G. J., and Siuzdak, G. (2012) An accelerated workflow for untargeted metabolomics using the METLIN database, *Nature biotechnology 30*, 826-828.